Heliyon 5 (2019) e02183

Contents lists available at ScienceDirect

Heliyon

journal homepage: www.heliyon.com

Heliyon

Supported ionic liquids as highly efficient and low-cost material for CO_2/CH_4 separation process

Bárbara B. Polesso [a], Franciele L. Bernard [b], Henrique Z. Ferrari [b], Evandro A. Duarte [b], Felipe Dalla Vecchia [a,b,c], Sandra Einloft [a,b,*]

[a] Post-Graduation Program in Materials Engineering and Technology, Pontifical Catholic University of Rio Grande do Sul – PUCRS, Brazil
[b] School of Technology, Pontifical Catholic University of Rio Grande do Sul – PUCRS, Brazil
[c] Institute of Petroleum and Natural Resources, Pontifical Catholic University of Rio Grande do Sul – PUCRS, Brazil

ARTICLE INFO

Keywords:
Petroleum engineering
CO_2 separation
Natural gas
Ionic liquids
Immobilization

ABSTRACT

Physical immobilization of ionic liquids (ILs) in solid materials appears as an interesting strategy for the development of new sorbents for CO_2 separation from natural gas. In this work the effect of physical immobilization of two ionic liquids with different anions (bmim[Cl] and bmim[OAc]) on two mesoporous supports (commercial silica SBA-15 and silica extracted from rice husk) was evaluated for CO_2 separation from natural gas by experimental determination of CO_2 sorption, CO_2/CH_4 selectivity and sorption kinetics. Results showed that the pure supports present the greatest CO_2 sorption capacity when compared to immobilized ILs. However, CO_2 removal efficiency improves considerably in the CO_2/CH_4 mixture when ILs are immobilized in these supports. The best selectivity results were obtained for supports immobilized with the IL bmim[Cl] and values increased for SIL-Cl by 37% and SBA-Cl 51% when compared with their respective supports. The contribution of SIL-Cl (3.03 ± 0.12) to separation performance (CO_2/CH_4) is similar to SBA-Cl (3.29 ± 0.39). ILs supported also presented fast sorption kinetics when compared to pure ILs thus being an interesting alternative in the search for highly efficient and low-cost separation processes.

1. Introduction

Natural gas (NG) is the fastest growing energy source being used nowadays and likely to grow for the next 20 years (Kang et al., 2017). Natural gas, an abundant and cleaner energy source is an alternative to oil and coal (Campos et al., 2017). Crude natural gas is mainly composed of methane presenting impurities (CO_2, H_2O, H_2S, etc) that must be removed to ensure process and transport specifications (Kang et al., 2017; Rufford et al., 2012; Song et al., 2017). Carbon dioxide is considered the main greenhouse gas (Jedli et al., 2018). Nowadays CO_2 concentration in atmosphere has increased by 40% when compared to pre-industrial era (IPCC, 2014; Mizuta et al., 2017). CO_2 removal is essential to prevent pipes and equipment corrosion in the presence of moisture and reduce transport cost (Kang et al., 2017; Song et al., 2017). Alkaloamines aqueous solutions is the most widely used technique for separating CO_2 from natural gas (Pino et al., 2016; Pongstabodee et al., 2016). However, it presents some drawbacks such as high cost for requiring large equipment and high energy to regenerate, chemical and oxidative degradation by the reaction with impurities, in addition to producing corrosive products (Huang et al., 2018; Kothandaraman et al., 2009; Thouchprasitchai et al., 2017; Ünveren et al., 2017). Ionic liquids (ILs) have aroused interest as substituents for conventional solvents, mainly due to the good selectivity towards CO_2 when compared with other gases. Yet, ILs are more versatile and less harmful to the environment than conventional organic solvents (Almantariotis et al., 2017; Anthony et al., 2002; Bara et al., 2009; Hanamertani et al., 2018, 2017; Hasib-ur-Rahman et al., 2010). ILs also present disadvantages such as high cost and viscosity, and low mass transfer in sorption process when compared to usual solvents (Safiah et al., 2014). In order to solve these problems, sorbent (e.g., amines, ionic liquids) immobilization in porous supports is an interesting alternative in CO_2 adsorption processes. Immobilization process can be performed by different routes: chemical or physical (Huang et al., 2017a; Peng et al., 2018). Impregnation process is carried out without chemical bonds formation and depends on sorbent affinity with the support surface. The anchorage and the sol-gel techniques are chemical immobilizations. In both cases, the contact between sorbent and support occurs through chemical bonding (Haber et al., 1995; Mäki-Arvela et al., 2006; Mehnert et al., 2002; Zhu et al., 2018).

* Corresponding author.
E-mail address: einloft@pucrs.br (S. Einloft).

https://doi.org/10.1016/j.heliyon.2019.e02183
Received 10 December 2018; Received in revised form 9 July 2019; Accepted 25 July 2019

Recent works with amine-impregnated adsorbents showed a potential for CO_2 capture (Huang et al., 2017a, 2018; Liu et al., 2017; Peng et al., 2018), but also presented intrinsic shortcomings such as solvent loss (due to high volatility), degradation and amine toxicity (Mohamedali et al., 2019). Literature describes the use of sorbents and support-immobilized ILs for CO_2 separation of gas streams from combustion gases and natural gas purification (Nanda et al., 2016; Sayari et al., 2011; Ünveren et al., 2017). Mesoporous silica, such as SBA-15, presents interesting properties for CO_2 separation as high pore volume and diameter, surface area and thermal stability (Guillet-Nicolas et al., 2017; Jahandar Lashaki et al., 2017; Jahandar Lashaki and Sayari, 2018; Selvakannan et al., 2013; Vilarrasa-Garcia et al., 2015). Recently, we have compared different anions ($[Cl]^-$; $[PF_6]^-$; $[Tf_2N]^-$; $[BF_4]^-$) for CO_2 sorption using imidazolium-based IL immobilized in MCM-41. Unlike the IL pool, where $[Tf_2N]^-$ is the best anion, the $[Cl]^-$ anion exhibited superior performance in the immobilized system (Aquino et al., 2015). Zhu et al. (2018) reported that the physical immobilization method of ILs on silica provided a greater selectivity when compared to pure silica and the IL immobilized by the anchorage method. Arellano et al. (2016) described that sorption kinetics of zinc-functionalized IL immobilized in SBA-15 support improved due to the increasing of available active sites.

Silica obtained from residues of rice milling also appears as potential materials for CO_2 capture representing both an environmental and low-cost option (Bhagiyalakshmi et al., 2010; Duczinski et al., 2018; Jang et al., 2009). We reported (Duczinski et al., 2018) that sorption capacity of immobilized samples by anchoring technic is lower than pure silica, whereas the CO_2/CH_4 selectivity increases 1.22 times for the sample with 10 wt. % immobilized IL. Moya et al. (2016) used wet impregnation method to encapsulate IL in aluminum silicates. The method ensured good distribution and pore filling of IL in the material. In this sense, the immobilization of ionic liquids in solid supports combines the advantages of ionic liquids with the characteristics of the porous supports.

In this work, we experimentally evaluated the main issues related to impregnation technique. The best combination among support and ionic liquid for CO_2 separation from natural gas were determined using the wet impregnation method. Parameters such as CO_2 sorption capacity, CO_2/CH_4 selectivity and sorption kinetics were evaluated using two ionic liquids with different anions ($[Cl]^-$ and $[OAc]^-$) and two types of mesoporous silica (commercial silica SBA-15 and rice husk extracted silica).

2. Experimental

2.1. Materials

1-Methylimidazole (99%, Sigma Aldrich), 1-Chlorobutane (99%, Sigma Aldrich), Acetone (99.5%, Vetec), Acetonitrile (99.0%, Merck), Toluene (99.0%, Merck), Methanol (99.8%, Merck), Hydrochloric acid (HCl, 32% Vetec), Dichloromethane (Anhydrol), Anhydrous Sodium Acetate (99%, Vetec), SBA-15 (99%, Sigma Aldrich) were used as received. The rice husk was donated by Cooperativa Arrozeira Extremo Sul Ltda. Ionic liquids [bmim][Cl] (1-butyl-3-methylimidazolium chloride) and [bmim][OAc] (1-butyl-3-methylimidazolium acetate) were synthesized as described elsewhere (Jain et al., 2005; Kiefer et al., 2008; Liu et al., 2011; Welton, 1999). Both samples were characterized by Fourier Transform Infrared Spectroscopy (FTIR) (Perkin Elmer Spectrum 100 FTIR spectrophotometer) using a fully attenuated reflectance (ATR) and by Proton Nuclear Magnetic Resonance (^{1}H-NMR) (Varian spectrophotometer, VNMRS 300 MHz), using DMSO-d_6 as solvent and 5 mm diameter glass tubes. [bmim][Cl]: ^{1}H-NMR (300 MHz, DMSO-d_6, 25 °C), δ (ppm) 1.01 (m, CH_3), 1.29 (m, CH_2CH_3), 1.83 (m, CH_2), 3.97 (s, CH_3), 4.25 (t, CH_2N), 7.79 (s, H_5), 7.91 (s, 9.48 (s, H_2). FTIR ν(cm^{-1}), 3143 (imidazole NH), 3073 (imidazole CH), 2936 (CH of CH_2), 2872 (CH of CH_3), 1634 (C–N imidazole), 1569-1430 (C–C and C–N imidazole), 755 (Cl^-). [bmim][OAc]: ^{1}H-NMR (300 MHz, DMSO-d_6, 25 °C), δ (ppm) 0.89 (t, CH_3, butyl), 1.22 (q, CH_3CH_2, butyl),1.62 (s, CH_3, acetate), 1.77 (t, N–CH_2–CH_2, butyl), 3.84 (s, N–CH_3), 4.15, N–CH_2), 7.68 (t, CH), 7.75 (t, CH), 9.24 (s, CH). FTIR ν (cm^{-1}) 3146 (NH, imidazole), 3086 (CH, imidazole), 2936 (CH of CH_2), 2874 (CH of CH_3), 1566 (C=O, acetate), 1566-1463 (C–C, C–N, imidazole, CH_2 of CH_3), 1463-1392 (C–H), 1334-1233 (CO, acetate), 1170-1112 (C–H_3), 1030-912 (CH).

2.2. Silica extraction from rice husk

Rice husk silica extraction was performed by acid hydrolysis (Bakar et al., 2016; Duczinski et al., 2018). First, rice husk was washed with distilled water to remove impurities and then mixed with 10% hydrochloric acid solution in the weight ratio of 1:9 (rice husk/solution) and kept for 2 hours in an autoclave at 125 °C. The autoclave content was washed with water to reach neutral pH and dried for 24 hours in an oven at 100 °C. After, the hydrolyzed rice husk was calcined in a muffle at 550 °C for 2h and silica obtained. The product was characterized by Fourier Transform Infrared (FTIR) spectroscopy by Perkin Elmer Spectrum 100 FTIR spectrophotometer with UATR. Four adsorption peaks appeared: two small peaks at 3357 cm^{-1} and 1634 cm^{-1} (attributed to the O–H elongation and vibration bending of adsorbed water) and two intense peaks corresponding to silica at 1051 and 798 cm^{-1} (Si–O–Si elongation and flexural vibrations).

2.3. ILs physical immobilization

Ionic liquids [bmim][Cl] and [bmim][OAc] immobilization on rice husk silica (SIL) and in commercial silica (SBA-15) was carried out by wet method (Haber et al., 1995). IL (10% in weight relative to silica) was dissolved in a small amount of dichloromethane (solvent) and added dropwise to the dried support. The homogenization was carried out manually using a pistil. After impregnation the solvent was removed in an oven at 120 °C for 1 hour (see Fig. 1).

2.4. CO_2 sorption and sorption Kinects tests

CO_2 solubility in porous supports was statically evaluated through pressure decay method in an equilibrium cell (Koros and Paul, 1976). The system consists of a double compartment cell (sample and gas tank). The tests were performed in triplicate. Initially, each sample (0.6–1.0 g) was oven dried at 65 °C for at least 2h to eliminate moisture. The sample was introduced into the sample compartment and CO_2 pressurized into the gas compartment. When the system reaches the desired temperature, the gas compartment is opened and CO_2 contacts the sample for the required time to achieve thermodynamic equilibrium. The amount of CO_2 adsorbed by the samples was calculated as described in literature (Bernard et al., 2017). Tests were carried out with pressure ranging from 0.06 to 1.5 MPa and temperatures of 25–45 °C. The solid sorption kinetics were evaluated by measuring the adsorbed amount over time. Recycle tests were performed by repeating the sorption/desorption cycles ten times at 0.4 MPa with desorption carried out after each cycle by heating the sample in an oven at 65 °C. The kinetics assays for pure ionic liquids were performed in a constant volume equilibrium cell with sapphire windows and the calculations performed by the isochoric saturation method (Jacquemin et al., 2006). The kinetics tests were performed under the same conditions as for the solids under constant stirring at 500 rpm.

2.5. CO_2/CH_4 separation – selectivity tests

Selectivity tests were performed using the same method described for CO_2 adsorption tests. The introduced gas into the gas compartment was a binary mixture of CO_2/CH_4 (35 mol % of CO_2 and CH_4 balance). Experiments were performed at 25 °C and equilibrium pressure of 2 MPa. The efficiency of the carbon dioxide separation was evaluated by CO_2 selectivity over CH_4 and calculated from the mole fractions in the gas phase (Y_i) and in the adsorbed phase (X_i), as shown in Eq. (1):

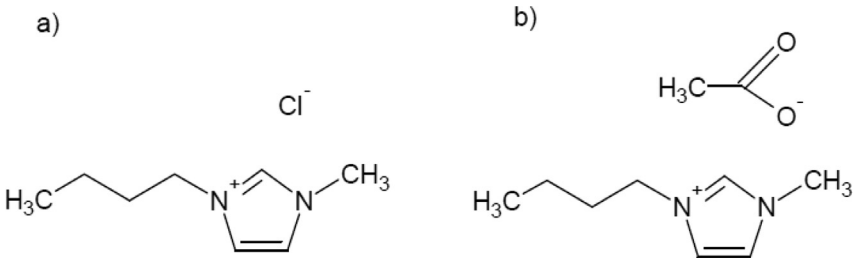

Fig. 1. Structure of imidazolium-based ionic liquids: a) [bmim][Cl] and b) [bmim][OAc].

$$S = \frac{XCO_2/YCO_2}{XCH_4/YCH_4} \quad (1)$$

The adsorbed molar fractions phase were calculated as described in detail by Azimi and Mirzaei (2016), referred to the non-adsorbed phase data obtained by gas chromatography using a thermal conductivity detector (GC-2014ATFSPL Shimadzu).

2.6. Samples characterization

The porous sample nature was investigated by N_2 adsorption-desorption technique and specific surface area was calculated using Brunauer – Emmett-Teller method (BET). Morphology was evaluated by scanning electron microscopy with field emission (SEM-FEG) using FEI Inspect F50 in the secondary electron mode (SE). Chemical composition was evaluated by energy dispersion X-ray spectrometry (EDS). For this purpose, samples were covered with a thin layer of gold. X-ray diffraction pattern (XRD) was recorded on Shimadzu XRD-700 equipment using Cu Kα radiation, voltage of 40 kV, 30 mA (1.5418 Å) ranging from 2 to 70° with scanning speed of 4°/min. Samples thermal stability and the immobilized ionic liquid actual content were evaluated by TGA/DTG (TA Instruments SDT-Q600), under nitrogen atmosphere within the range from 25 to 800 °C and heating rate of 20 °C/min. All analyses were conducted in triplicate. The IL loading in silica support (denoted as IL%) was calculated from the TGA curve using the following Eq. (2):

$$IL\ (\%) = \frac{W_{150} - W_{800}}{W_{150}} \times 100 \quad (2)$$

Where, W_{150} and W_{800} are sample weight (g) at 150 °C and 800 °C, respectively.

3. Results and discussion

3.1. Textural properties

Table 1 presents the specific surface area and pore size values of the pure and immobilized supports with the respective ionic liquids. SBA presented the largest specific surface area (762 m^2/g), pore volume (1.62 cm^3/g) and pore radius (7.20 nm) when compared to SIL (S = 246 m^2/g, Vp = 0.32 cm^3/g and Rp = 3.88 nm).

ILs immobilization resulted in specific surface area and pore volume values reduction up to 50% for SBA samples. These results evidenced that the porous materials surface was covered with IL. Yet, pores were probably filled, as already reported (Aquino et al., 2015; Arellano et al., 2016; Nkinahamira et al., 2017; Safiah et al., 2014). For SIL samples a small reduction was observed. Fig. 2 shows pore distribution evidencing that after ILs immobilization the SBA samples decreased pore radius suggesting the IL immobilization occurred in SBA channels (Zou et al., 2010). Unlike the SBA, SIL samples showed similar pore radius distribution after IL immobilization. This behavior evidences the influence of textural properties of supports in IL organization after immobilization process.

Table 1
Structural properties of supports and ionic liquid supported.

Sample	S_{BET} (m^2/g)	V_p (cm^3/g)	R_p (nm)
SIL	246	0.32	3.88
SIL-Cl	164	0.23	3.88
SIL-OAc	165	0.25	3.11
SBA	762	1.62	7.20
SBA-Cl	491	0.79	5.07
SBA-OAc	399	0.76	5.07

3.2. Thermogravimetric analysis

IL immobilized amount in the supports was estimated by TGA (Fig. 3: Fig. 3a corresponding to SIL and ILs immobilized in SIL, Fig. 3b corresponds to SBA and ILs immobilized in SBA and Fig. 3c the pure ionic liquids). The mass loss observed up to 150 °C corresponds to water loss. The mass loss of supports without IL and the T_{onset} of pure ILs were evaluated in order to understand the immobilized ILs behavior ($T_{onset\ [bmim][Cl]}$ = 272 °C; $T_{onset[bmim][OAc]}$ = 242 °C). The mass loss for SIL was 1.85% and for SBA-15 1.37%, meaning that the support materials are thermally stable in the evaluated range. Mass loss of immobilized ILs SIL-Cl, SIL-OAc SBA-Cl and SBA-OAc represented 10.15%, 8.75, 9.91%, and 11.2%, respectively, meaning that the actual amount of immobilized IL was 8.30% (±0.07), 6.90% (±0.20), 8.54% (±0.96) and 9.83% (±0.17), respectively. Experimental results are close to immobilized IL theoretical values (10%) evidencing that the wet method is efficient.

3.3. Morphological analysis and chemical composition

Fig. 4 presents the micrograph images of SIL (a) and SBA (d) supports and the ILs immobilized in these supports (SIL-Cl (b); SIL-OAc (c); SBA-Cl (e); SBA-OAc (f)) as well as their respective EDS spectra indicated by the corresponding letter and subscript 1.

Silica extracted from rice husk (SIL) micrographs (Fig. 4a) exhibited spherical/semi-spherical particle agglomerates in certain regions (Jung et al., 2013; Sankar et al., 2016). This behavior is also observed in samples with immobilized IL (Fig. 4b and c). Commercial silica SBA micrographs (Fig. 4d) evidenced the existence of macro-structures similar to grains with a pore length of 1339 μm (Cheng et al., 2018; Kalita and Kumar, 2011; Sawant et al., 2005). After ILs immobilization samples SBA-Cl (Fig. 4e) and SBA-OAc (Fig. 4f) showed a similar particle morphology with pore length close to the support (1331 μm and 1344 μm, respectively). The similar behavior presented before and after ILs immobilization in both supports reflects stabilized support macroscopic structure (Kalita and Kumar, 2011). EDS analysis was used to confirm the ILs immobilization by the presence of the chemical compounds corresponding to each sample (support and ILs) (Cheng et al., 2018). The presence of gold in all spectra corresponds to the metallization required to perform the analysis. For supports as shown in Fig. 4a_1 and 4d_1 only silicon and oxygen, characteristic of silica, were observed. For samples immobilized with bmim [Cl] the additional presence of chlorine and carbon, characteristic of this IL, was observed

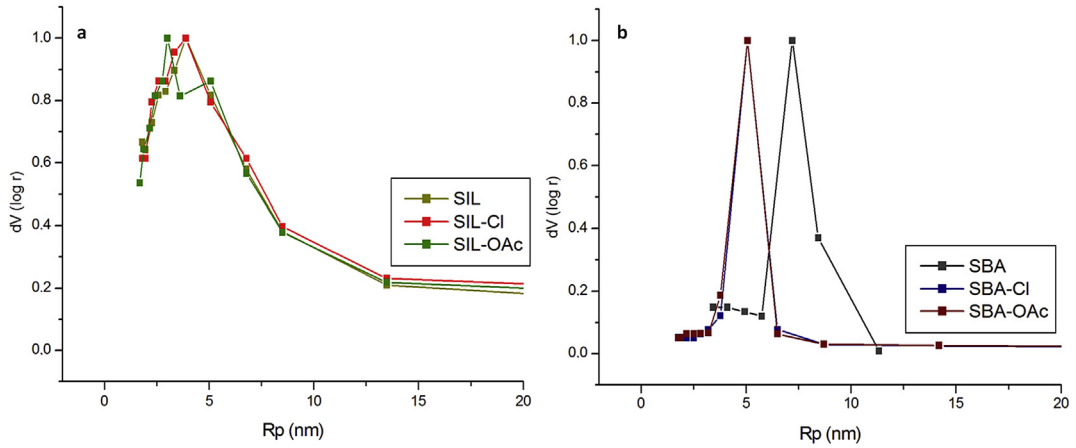

Fig. 2. Pore distribution of (a) SIL and immobilized ILs (b) SBA and immobilized ILs.

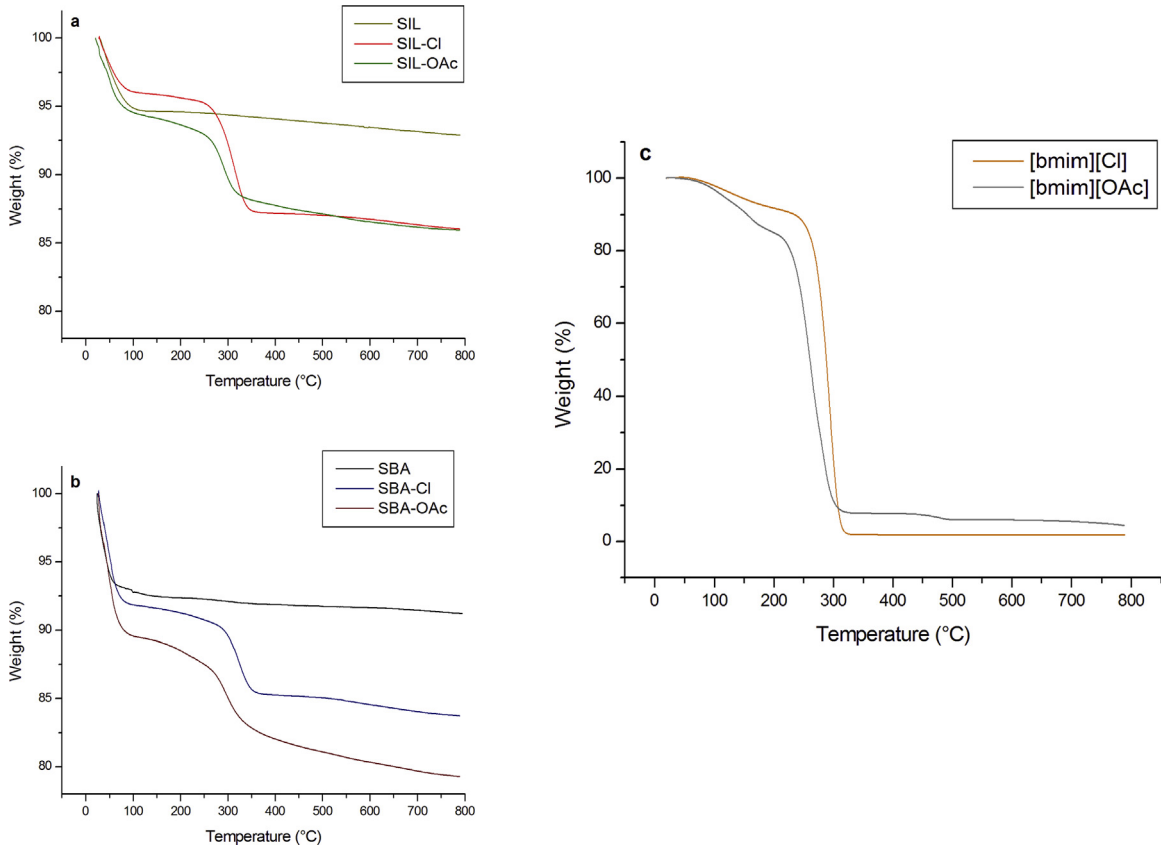

Fig. 3. Thermogravimetric analysis of: (a) SIL and immobilized ILs (b) SBA and immobilized ILs and (c) pure ILs.

(Fig. 4b$_1$ and 4e$_1$). For samples immobilized with bmim [OAc] (Fig. 4c$_1$ and 4f$_1$) only carbon was observed besides oxygen and silicon. These results evidenced that the ILs were successfully immobilized on the support materials.

3.4. XRD analysis

XRD sample patterns are shown in Fig. 5 (5a shows the SIL samples and 5b SBA samples). The supports are completely amorphous as indicated by the diffractograms and the appearance of a slight peak at $2\theta \approx 22^{\circ}$, typical of amorphous silica (Bakar et al., 2016; Barros et al., 2013). After ILs immobilization, materials showed XRD patterns similar to the supports indicating that the support structure was preserved (Xie et al., 2015).

3.5. CO_2 sorption tests

Fig. 6 shows sorption values for supports as well as for ILs supported in both SIL and SBA. Sorption tests were performed at 25 °C and 0.4 MPa of equilibrium pressure. It is possible to observe that the silica supports (SIL and SBA) have a high CO_2 sorption capacity (73.8 mg CO_2/g and 125.8 mg CO_2/g, respectively). Sorption values are lower after IL immobilization due to IL surface recovering, decreasing specific surface area and pore volume after immobilization (Duczinski et al., 2018; Ren et al., 2012). Comparing the two supports, one can see that the commercial silica SBA shows greater sorption capacities. This behavior is

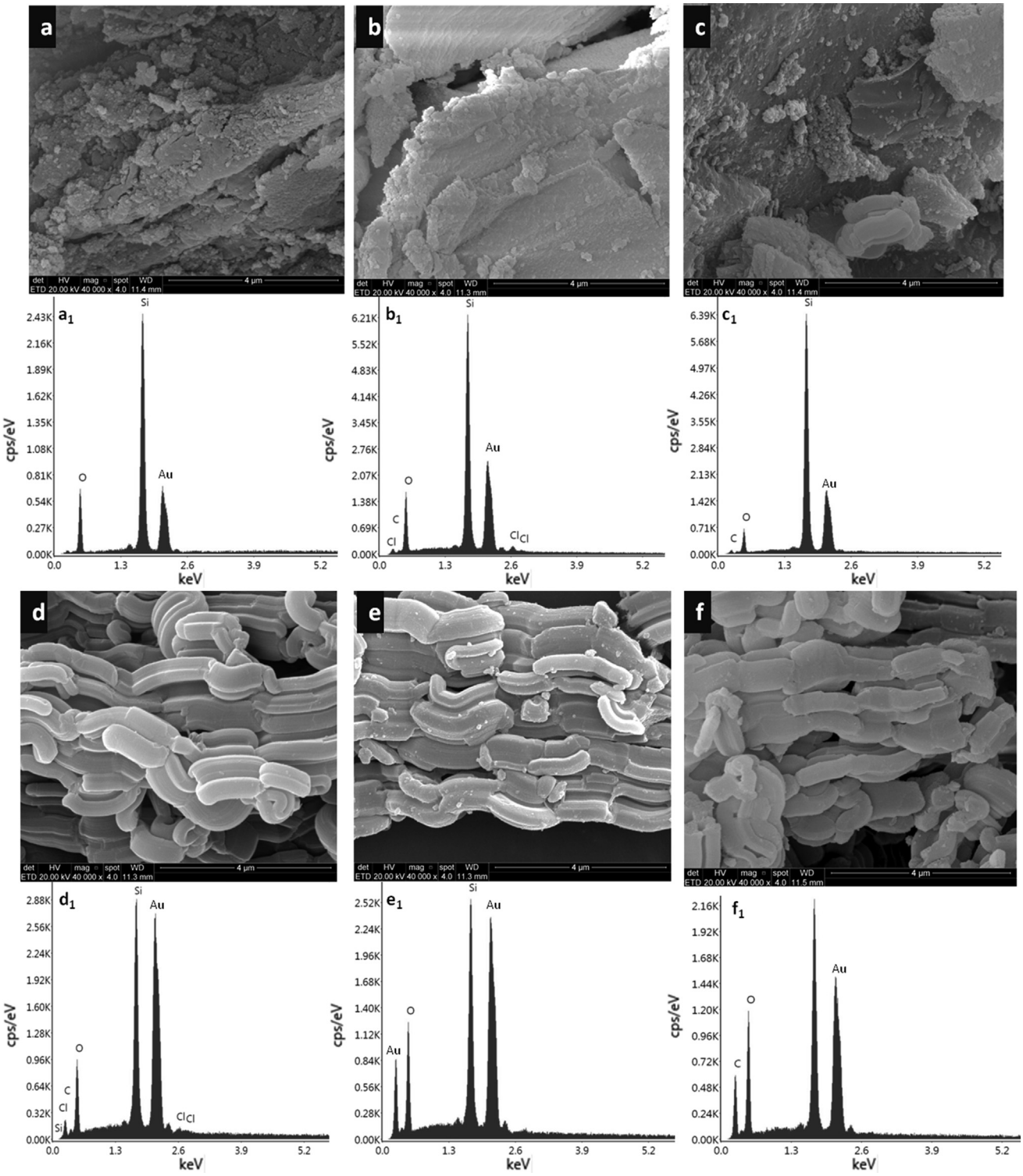

Fig. 4. Field emission scanning electron micrographs: (a) SIL (b) SIL-Cl (c) SIL-OAc (d) SBA (e) SBA-Cl (f) SBA-OAc and EDS: (a_1) SIL (b_1) SIL-C; (c_1) SIL-OAc (d_1) SBA (e_1) SBA-Cl (f_1) SBA-OAc.

probably associated to larger specific surface area and pore volume when compared to SIL sample (Zhu et al., 2014) as presented in Table 1. The drawback of this support is the high cost (5g U$D 139.00- Sigma-Aldrich) thus discouraging its use. Fig. 7 presents IL loading versus CO_2 sorption capacity. In SBA-15 support the [bmim] [Cl] loading amount was similar to [bmim][OAc] whereas in SIL the [bmim] [Cl] loading amount was superior than [bmim][OAc].It can be seen from Fig. 6 that highest CO_2 adsorption results were obtained for [bmim][OAc] in both SIL and SBA. These results suggest that the nature of anion has a large effect on gas solubility as reported in literature (Anthony et al., 2005). The anion [OAc]- confers a greater sorption capacity on the immobilized samples (SIL-OAc 54.8 mgCO_2/g, SBA-OAc 105.2 mgCO_2/g) when compared to $[Cl]^-$ (SIL-Cl 47.2 mg CO_2/g, SBA-Cl 98.9 mgCO_2/g). IL [bmim][OAc] presents a higher CO_2 sorption capacity when compared to [bmim][Cl] as reported by Yim et al. (2018). This result is related to chemical absorption capacity of CO_2 by the IL [bmim][OAc]. In this case CO_2 reacts

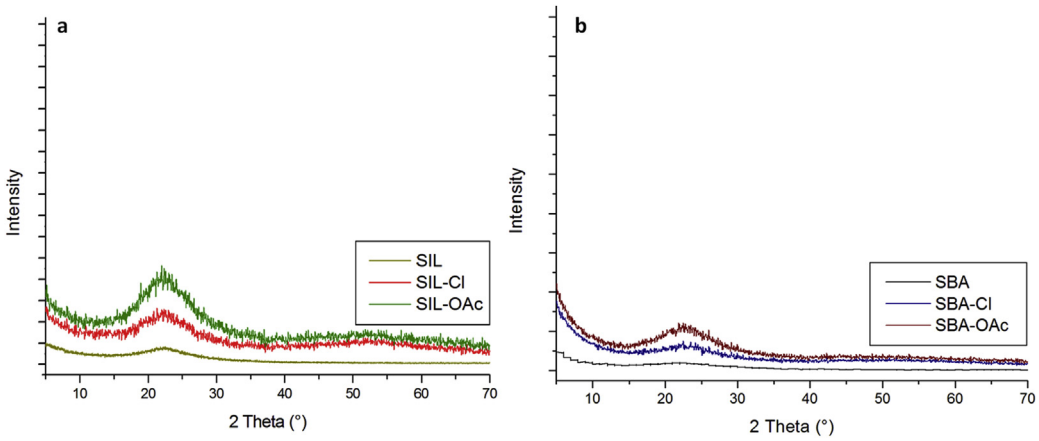

Fig. 5. XRD sample patterns: (a) SIL, SIL-Cl and SIL-OAc samples (b) SBA, SBA-Cl and SBA-OAc.

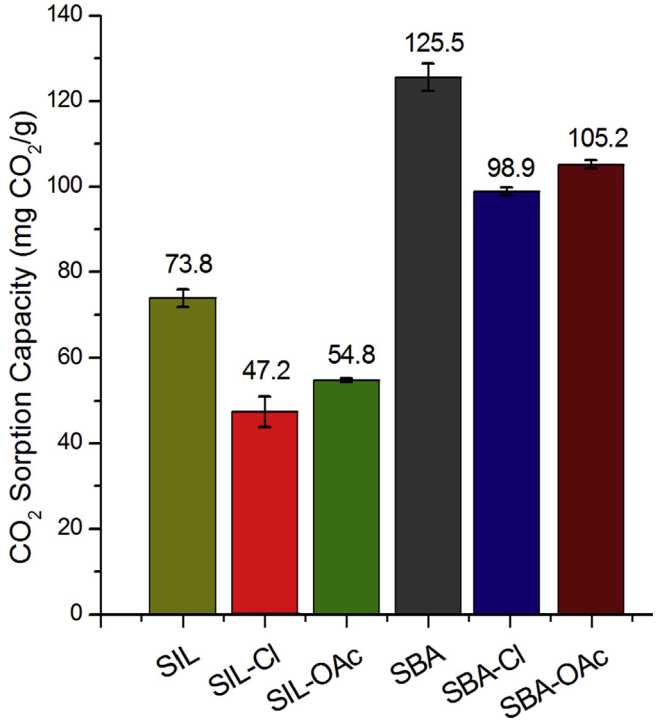

Fig. 6. CO_2 sorption capacity of silica supports with and without immobilized ionic liquids.

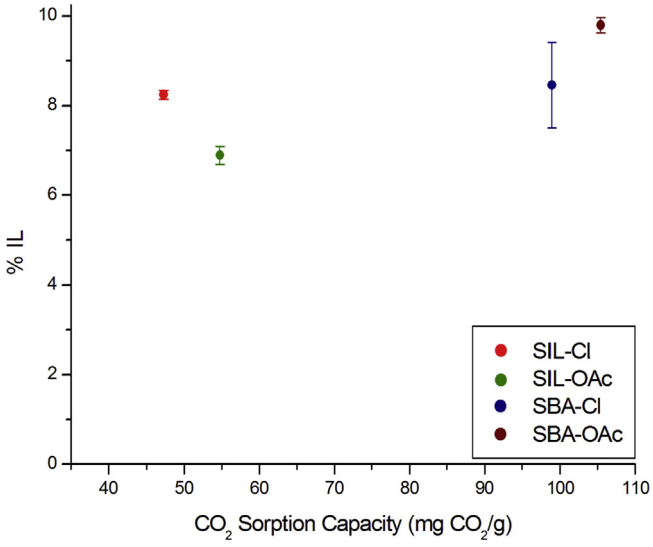

Fig. 7. IL loading amount versus CO_2 sorption capacity.

with the imidazolium ring cation forming carboxylate thus increasing CO_2 absorption capacity (Chen et al., 2011; Moya et al., 2016; Zareiekordshouli et al., 2018; Ziobrowski et al., 2016).

Table 2 presents a comparison among literature results for CO_2 sorption capacity and results obtained in this work. As we can see the result obtained with SIL-extracted from rice husk is similar to commercial zeolites and superior when compared to synthesized MCM-48 and commercial MCM-41 in similar pressure and temperature conditions. These results demonstrated that the IL immobilization in silica support obtained from agriculture waste appears as an alternative option for CO_2 separation process.

3.6. Kinects tests

Regarding the kinetic behavior, Fig. 8 shows a comparison of the CO_2 sorption time at 25 °C and 0.4 MPa for solid supports as well as for the ILs immobilized in the supports (Fig. 8a). Fig. 8 (8b) also includes CO_2 sorption kinetics of the two ILs [bmim][OAc] and [bmim] [Cl] and represents a function of q/qe vs t, where q corresponds to the quantity of CO_2 absorbed at time t; qe, the amount of CO_2 corresponding to saturation; and t, the time required to saturate. Table 3 summarizes the values corresponding to $t_{0.9}$, ie, the time at which 90% of the CO_2 sorption capacity is reached.

Ionic liquids physical immobilization drastically improves CO_2 sorption kinetics as compared with ILs. The time to reach 90% of the sorption capacity has dropped from approximately 2 hours to a maximum of 5 minutes. This behavior is associated with ILs high viscosity difficulting mass transfer. When ILs are immobilized in a solid support an increase of gas-liquid contact area is reached, improving kinetic to supported materials as previously reported (Aboudi and Vafaeezadeh, 2015; Moya et al., 2016; Safiah et al., 2014; Yang and Wang, 2015). The same behavior was evidenced for 1-Butyl-methylimidazolium acetate encapsulated in a solid material. The encapsulation increased the CO_2 sorption rate from 20h ([bmim][OAc]) to less than 20 min at 1 bar and 303 K (Moya et al., 2016).

3.7. CO_2/CH_4 selectivity

As depicted in Fig. 9 CO_2/CH_4 separation selectivity is improved with ILs immobilization when compared to SIL and SBA supports. ILs shows more affinity for CO_2 when compared to other gases such as CH_4 and N_2

Table 2
Comparison of different CO_2 sorbents.

Adsorbent	Support Material	%Theoretical Load	CO_2 Sorption capacity (mg/g)	P (MPa)	T (°C)	Reference
MCM-48-35PEHA-15DEA	MCM-48	50	25.52	0.4	25	(Anbia et al., 2012)
$ILBF_4M50$	MCM-41	50	20.00	0.4	25	(Aquino et al., 2015)
$ILPF_6M50$	MCM-41	50	44.00	0.4	25	(Aquino et al., 2015)
$ILTf_2NM50$	MCM-41	50	20.00	0.4	25	(Aquino et al., 2015)
bmimAc@ZIF-10	Zeolite (ZIF8)	10	49.94	0.4	30	(Mohamedali et al., 2018)
emimAc@ZIF-10	Zeolite (ZIF8)	10	47.96	0.4	30	(Mohamedali et al., 2018)
SIL-Cl	SIL	10	47.20	0.4	25	(This work)

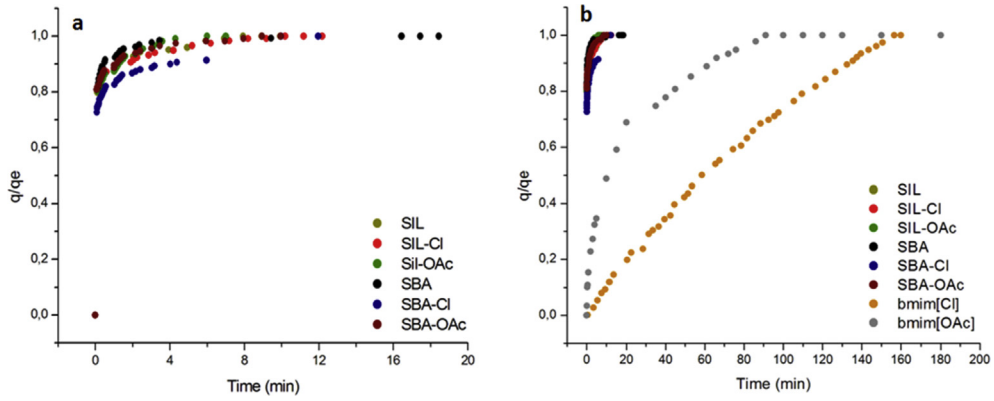

Fig. 8. Sorption time of: (a) Supports and immobilized ILs (b) Supports, immobilized and pure ILs.

Table 3
Time at which 90% of the CO_2 sorption capacity is reached.

Sample	$t_{0.9}$ (min)
SIL	1.3
SIL-Cl	1.9
SIL-OAc	1.2
SBA	0.5
SBA-Cl	4.0
SBA-OAc	1.1
bmim [Cl]	135
bmim [OAc]	65

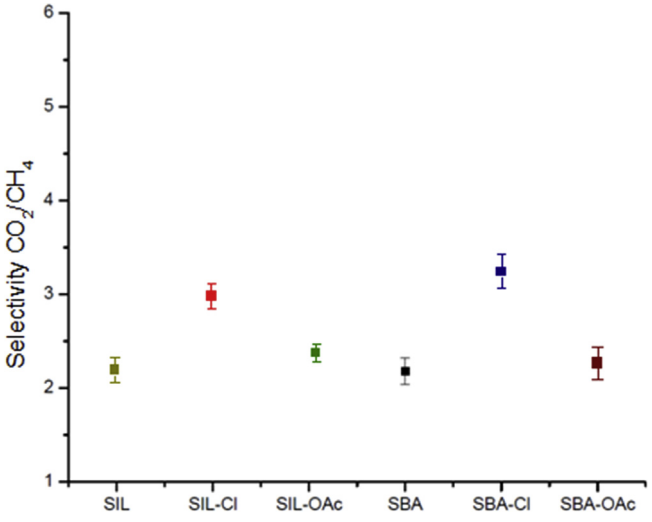

Fig. 9. Silica supports selectivity with and without immobilized ionic liquids.

(Anthony et al., 2005). Acidic hydrogen from imidazolium ring exhibit affinity to CO_2 and does not exhibit any affinity to CH_4 thus improving selectivity (Duczinski et al., 2018). Yet, ILs polar nature, mainly associated with the imidazolium cation, improves selectivity (Hojniak et al., 2014; Salehi and Anbia, 2017). The best selectivity results were obtained for supports immobilized with the IL bmim [Cl] and values increased for SIL-Cl by 1.37 times and for SBA-Cl 1.51 times when compared with their respective supports. Although similar results have been obtained with commercial silica SBA-Cl (3.29 ± 0.39) and SIL-Cl (3.03 ± 0.12), it is important to remember that SBA is a high cost material. The chloride overperforms acetate in CO_2/CH_4 because it is relatively small (as compared to acetate) and strongly interacts with imidazolium cation leaving support binding sites available for CO_2 (Aquino et al., 2015). The good result obtained with SIL-Cl must be highlighted once imidazolium chloride is a precursor for acetate ILs (Aquino et al., 2015; Duczinski et al., 2018). Compare imidazolium Cl price (5g U$D 54.1, Sigma-Aldrich) with imidazolium acetate price (5g U$D 124.00, Sigma-Aldrich). When comparing to amines imidazolium based IL are expensive. Nevertheless, this comparison is estimated based on laboratory-scale syntheses. Support material is obtained from waste and is assumed low cost reducing sorbent costs. Further benefits can include IL/support properties when compared to amines such as low volatility and low solvent loss. Yet, ILs are stable and used in low concentration (10% in weight relative to silica). Obtained CO_2/CH_4 selectivity value for SIL-Cl sample (~3.0) is higher than those repported in literature under the same pressure and temperature conditions for a metal-organic framework (~2.5) (Yang and Zhong, 2006).

3.8. *Influence of temperature and pressure on CO_2 sorption capacity*

SIL, SIL-Cl and SIL-OAc were selected to evaluate the influence of temperature and pressure on CO_2 sorption due to CO_2/CH_4 selectivity performance and low cost when compared to SBA samples. Temperature (25–45 °C at 0.4 MPa) and pressure (0.06–1.5 MPa at 25 °C) effect were evaluated in CO_2 sorption capacity (Fig. 10a and b). The results shown in Fig. 10a indicated two different behaviors. For SIL and SIL-Cl samples an increase in temperature resulted in a decrease on CO_2 sorption capacity, indicating typical behavior of a physical sorbent. Similar behavior was described in litertura (Bernard et al., 2019; Ye et al., 2012). For SIL-OAc

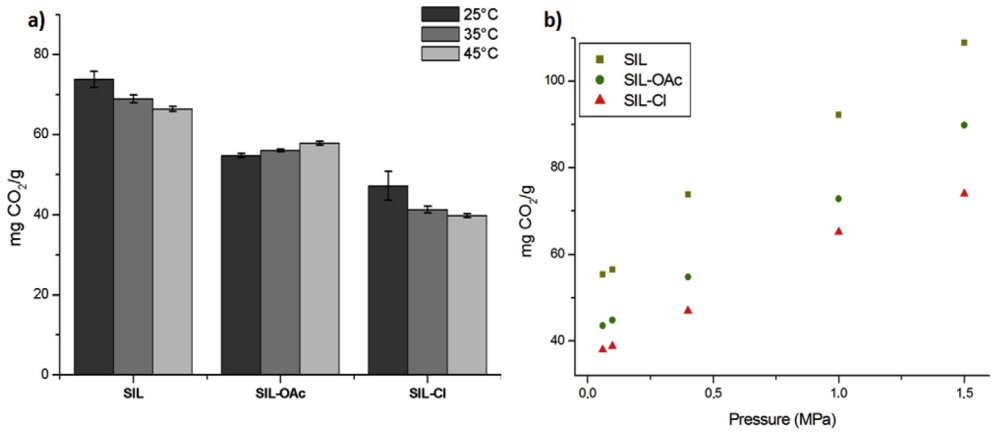

Fig. 10. (a) Effect of temperature at 0.4 MPa (b) Effect of pressure at 25 °C.

the temperature increase improves the interaction between $[OAc]^-$ and CO_2 molecules increasing CO_2 sorption capacity. This result suggests a physical and chemical sorption (Huang et al., 2017b; Ye et al., 2012).

Fig. 10b demonstrated that gas sorption capacity increases with CO_2 partial pressure increses. SIL sample presented higher CO_2 sorption capacity probably associated to larger specific surface area and pore volume (Table 1). When comparing the performance of immobilized ILs, SIL-OAc presented higher sorption capacity than SIL-Cl, suggesting that CO_2 sorption is occuring by both physical and chemical sorption.

3.9. Recycle tests

In order to verify sample stability after successive sorption/desorption cycles, recycle tests were performed in the most interesting sample in relation to CO_2 sorption capacity and, mainly, selectivity and cost. In this sense, sorption/desorption tests were performed in the SIL-Cl sample and the results presented in Fig. 11. After 10 sorption/desorption cycles, the sorption capacity obtained was almost unchanged thus confirming its stability and reuse.

4. Conclusions

Two ionic liquids with [bmim] cation were synthesized and immobilized on commercial silica and low-cost silica supports extracted from rice husk. ILs were immobilized on the supports by physical wet impregnation method. The sorbents retained the partial pore characteristics (due to specific surface area and pore volume reduction) directly influencing their sorption capacity. Although CO_2 sorption capacity decreases, CO_2 removal efficiency in the CO_2/CH_4 mixture (evaluated by the selectivity) improves considerably for samples with immobilized ILs, evidencing the influence of the IL and CO_2 affinity. Supported ILs showed fast sorption kinetics when compared to pure ILs. The results evidenced that IL physical immobilization represents an alternative to separation processes, being SIL-Cl the most interesting combination of support and ionic liquid since high selectivity and low-cost are essential parameters for the development of new materials for natural gas purification.

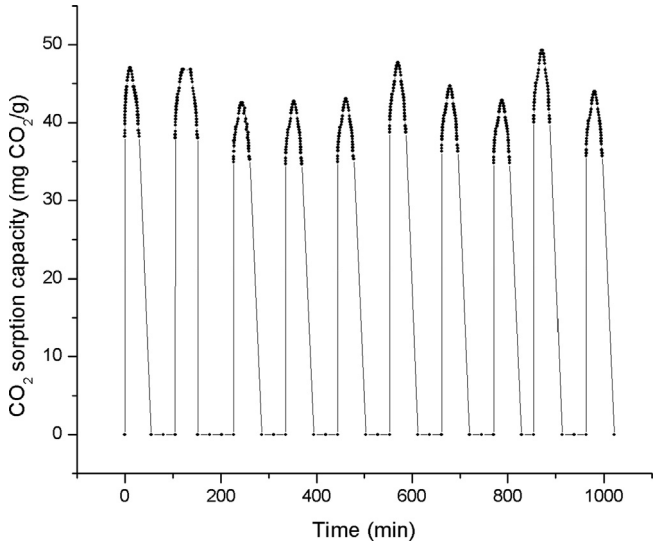

Fig. 11. Recycle test applied to the sample SIL-Cl. Conditions: 25 °C and 0.4 MPa.

Declarations

Author contribution statement

Bárbara Polesso: Conceived and designed the experiments; Performed the experiments; Analyzed and interpreted the data; Contributed reagents, materials, analysis tools or data; Wrote the paper.

Franciele Bernard: Conceived and designed the experiments; Analyzed and interpreted the data; Wrote the paper.

Henrique Ferrari, Evandro Duarte: Performed the experiments.

Felipe Dalla Vecchia: Conceived and designed the experiments; Analyzed and interpreted the data.

Sandra Einloft: Conceived and designed the experiments; Analyzed and interpreted the data; Contributed reagents, materials, analysis tools or data; Wrote the paper.

Funding statement

This work was supported by the Coordenação de Aperfeiçoamento de Pessoal de Nivel Superior – Brasil (CAPES) – Finance Code 001 and CNPq through a PQ grant.

Competing interest statement

The authors declare no conflict of interest.

Additional information

No additional information is available for this paper.

References

Aboudi, J., Vafaeezadeh, M., 2015. Efficient and reversible CO_2 capture by amine functionalized-silica gel confined task-specific ionic liquid system. J. Adv. Res. 6, 571–577.

Almantariotis, D., Pensado, A.S., Gunaratne, H.Q.N., Hardacre, C., Pádua, A.A.H., Coxam, J.Y., Costa Gomes, M.F., 2017. Influence of fluorination on the solubilities of carbon dioxide, ethane, and nitrogen in 1-n-fluoro-alkyl-3-methylimidazolium bis(n-fluoroalkylsulfonyl)amide ionic liquids. J. Phys. Chem. A 121, 426–436.

Anbia, M., Hoseini, V., Mandegarzad, S., 2012. Synthesis and characterization of nanocomposite MCM-48-PEHA-DEA and its application as CO2adsorbent. Korean J. Chem. Eng. 29, 1776–1781.

Anthony, J.L., Anderson, J.L., Maginn, E.J., Brennecke, J.F., 2005. Anion effects on gas solubility in ionic liquids. J. Phys. Chem. B 109, 6366–6374.

Anthony, J.L., Maginn, E.J., Brennecke, J.F., 2002. Solubilities and thermodynamic properties of gases in the ionic liquid 1-n-butyl-3-methylimidazolium hexafluorophosphate. J. Phys. Chem. B 106, 7315–7320.

Aquino, A.S., Bernard, F.L., Borges, J.V., Mafra, L., Vecchia, F.D., Vieira, M.O., Ligabue, R., Seferin, M., Chaban, V.V., Cabrita, E.J., Einloft, S., 2015. Rationalizing the role of the anion in CO_2 capture and conversion using imidazolium-based ionic liquid modified mesoporous silica. RSC Adv. 5, 64220–64227.

Arellano, I.H., Madani, S.H., Huang, J., Pendleton, P., 2016. Carbon dioxide adsorption by zinc-functionalized ionic liquid impregnated into bio-templated mesoporous silica beads. Chem. Eng. J. 283, 692–702.

Azimi, A., Mirzaei, M., 2016. Experimental evaluation and thermodynamic modeling of hydrate selectivity in separation of CO2and CH4. Chem. Eng. Res. Des. 111, 262–268.

Bakar, R.A., Yahya, R., Gan, S.N., 2016. Production of high purity amorphous silica from rice husk. Procedia Chem 19, 189–195.

Bara, J.E., Carlisle, T.K., Gabriel, C.J., Finotello, A., Gin, D.L., Noble, R.D., Camper, D., 2009. Guide to CO separations in imidazolium-based room-temperature ionic liquids guide to CO 2 separations in imidazolium-based room-temperature ionic liquids. Ind. Eng. Chem. Res. 2739–2751.

Barros, S.D.T., Coelho, A.V., Lachter, E.R., San Gil, R.A.S., Dahmouche, K., Pais da Silva, M.I., Souza, A.L.F., 2013. Esterification of lauric acid with butanol over mesoporous materials. Renew. Energy 50, 585–589.

Bernard, F.L., dos Santos, L.M., Schwab, M.B., Polesso, B.B., do Nascimento, J.F., Einloft, S., 2019. Polyurethane-based poly (ionic liquid)s for CO 2 removal from natural gas. J. Appl. Polym. Sci. 136, 4–11.

Bernard, F.L., Polesso, B.B., Cobalchini, F.W., Chaban, V.V., Do Nascimento, J.F., Dalla Vecchia, F., Einloft, S., 2017. Hybrid alkoxysilane-functionalized urethane-imide-based poly(ionic liquids) as a new platform for carbon dioxide capture. Energy Fuels 31, 9840–9849.

Bhagiyalakshmi, M., Yun, L.J., Anuradha, R., Jang, H.T., 2010. Utilization of rice husk ash as silica source for the synthesis of mesoporous silicas and their application to CO2adsorption through TREN/TEPA grafting. J. Hazard Mater. 175, 928–938.

Campos, A.F., da Silva, N.F., Pereira, M.G., Vasconcelos Freitas, M.A., 2017. A review of Brazilian natural gas industry: challenges and strategies. Renew. Sustain. Energy Rev. 75, 1207–1216.

Chen, Y., Han, J., Wang, T., Mu, T., 2011. Determination of absorption rate and capacity of CO2in ionic liquids at atmospheric pressure by thermogravimetric analysis. Energy Fuels 25, 5810–5815.

Cheng, J., Li, Y., Hu, L., Liu, J., Zhou, J., Cen, K., 2018. CO2absorption and diffusion in ionic liquid [P66614][Triz] modified molecular sieves SBA-15 with various pore lengths. Fuel Process. Technol. 172, 216–224.

Duczinski, R., Bernard, F., Rojas, M., Duarte, E., Chaban, V., Vecchia, F.D., Menezes, S., Einloft, S., 2018. Waste derived MCMRH- supported IL for CO 2/CH 4 separation. J. Nat. Gas Sci. Eng. 54, 54–64.

Guillet-Nicolas, R., Bérubé, F., Thommes, M., Janicke, M.T., Kleitz, F., 2017. Selectively tuned pore condensation and hysteresis behavior in mesoporous SBA-15 silica: correlating material synthesis to advanced gas adsorption analysis. J. Phys. Chem. C 121, 24505–24526.

Haber, J., Block, J.H., Delmon, B., 1995. Manual of methods and procedures for catalyst characterization (Technical Report). Pure Appl. Chem. 67, 1257–1306.

Hanamertani, A.S., Pilus, R.M., Idris, A.K., Irawan, S., Tan, I.M., 2017. Ionic liquids as a potential additive for reducing surfactant adsorption onto crushed Berea sandstone. J. Pet. Sci. Eng. 162, 480–490.

Hanamertani, A.S., Pilus, R.M., Manan, N.A., Mutalib, M.I.A., 2018. The use of ionic liquids as additive to stabilize surfactant foam for mobility control application. J. Pet. Sci. Eng. 167, 192–201.

Hasib-ur-Rahman, M., Siaj, M., Larachi, F., 2010. Ionic liquids for CO2capture-Development and progress. Chem. Eng. Process. Process Intensif. 49, 313–322.

Hojniak, S.D., Silverwood, I.P., Khan, A.L., Vankelecom, I.F.J., Dehaen, W., Kazarian, S.G., Binnemans, K., 2014. Highly selective separation of carbon dioxide from nitrogen and methane by nitrile/glycol-difunctionalized ionic liquids in supported ionic liquid membranes (SILMs). J. Phys. Chem. B 118, 7440–7449.

Huang, K., Liang, L., Chai, S., Tumuluri, U., Li, M., Wu, Z., Sumpter, B.G., Dai, S., 2017a. Aminopolymer functionalization of boron nitride nanosheets for highly efficient capture of carbon dioxide. J. Mater. Chem. A 5, 16241–16248.

Huang, K., Liu, F., Fan, J.P., Dai, S., 2018. Open and hierarchical carbon framework with ultralarge pore volume for efficient capture of carbon dioxide. ACS Appl. Mater. Interfaces 10, 36961–36968.

Huang, L., Zhang, Y., Gao, W., Harada, T., Qin, Q., Zheng, Q., Hatton, T.A., Wang, Q., 2017b. Alkali carbonate molten salt coated calcium oxide with highly improved carbon dioxide capture capacity. Energy Technol. 5, 1328–1336.

IPCC, 2014. Summary for Policymakers, Climate Change 2014: Synthesis Report. Contribution of Working Groups I, II and III to the Fifth Assessment Report of the Intergovernmental Panel on Climate Change.

Jacquemin, J., Costa Gomes, M.F., Husson, P., Majer, V., 2006. Solubility of carbon dioxide, ethane, methane, oxygen, nitrogen, hydrogen, argon, and carbon monoxide in 1-butyl-3-methylimidazolium tetrafluoroborate between temperatures 283 K and 343 K and at pressures close to atmospheric. J. Chem. Thermodyn. 38, 490–502.

Jahandar Lashaki, M., Sayari, A., 2018. CO2capture using triamine-grafted SBA-15: the impact of the support pore structure. Chem. Eng. J. 334, 1260–1269.

Jahandar Lashaki, M., Ziaei-Azad, H., Sayari, A., 2017. Insights into the hydrothermal stability of triamine-functionalized SBA-15 silica for CO2Adsorption. ChemSusChem 10, 4037–4045.

Jain, N., Kumar, A., Chauhan, S., Chauhan, S.M.S., 2005. Chemical and biochemical transformations in ionic liquids. Tetrahedron 61, 1015–1060.

Jang, H.T., Park, Y.K., Ko, Y.S., Lee, J.Y., Margandan, B., 2009. Highly siliceous MCM-48 from rice husk ash for CO2 adsorption. Int. J. Greenhouse Gas Control 3, 545–549.

Jedli, H., Brahmi, J., Hedfi, H., Mbarek, M., Bouzgarrou, S., Slimi, K., 2018. Adsorption kinetics and thermodynamics properties of Supercritical CO2 on activated clay. J. Pet. Sci. Eng. 166, 476–481.

Jung, D.S., Ryou, M.-H., Sung, Y.J., Park, S.B., Choi, J.W., 2013. Recycling rice husks for high-capacity lithium battery anodes. Proc. Natl. Acad. Sci. 110, 12229–12234.

Kalita, P., Kumar, R., 2011. Immobilization of 1,5,7-triazabicyclo [4.4.0] dec-5-ene over mesoporous materials: an efficient catalyst for Michael-addition reactions under solvent-free condition. Appl. Catal. Gen. 397, 250–258.

Kang, G., Chan, Z.P., Saleh, S.B.M., Cao, Y., 2017. Removal of high concentration CO2from natural gas using high pressure membrane contactors. Int. J. Greenhouse Gas Control 60, 1–9.

Kiefer, J., Obert, K., Bösmann, A., Seeger, T., Wasserscheid, P., Leipertz, A., 2008. Quantitative analysis of alpha-D-glucose in an ionic liquid by using infrared spectroscopy. ChemPhysChem 9, 1317–1322.

Koros, W.J., Paul, D.R., 1976. Design considerations for measurement of gas sorption in polymers by pressure decay. J. Polym. Sci., Polym. Phys. Ed. 14, 1903–1907.

Kothandaraman, A., Nord, L., Bolland, O., Herzog, H.J., McRae, G.J., 2009. Comparison of solvents for post-combustion capture of CO2 by chemical absorption. Energy Procedia 1, 1373–1380.

Liu, F., Huang, K., Yoo, C.J., Okonkwo, C., Tao, D.J., Jones, C.W., Dai, S., 2017. Facilely synthesized meso-macroporous polymer as support of poly(ethyleneimine) for highly efficient and selective capture of CO2. Chem. Eng. J. 314, 466–476.

Liu, F., Li, L., Yu, S., Lv, Z., Ge, X., 2011. Methanolysis of polycarbonate catalysed by ionic liquid [Bmim][Ac]. J. Hazard Mater. 189, 249–254.

Mäki-Arvela, P., Mikkola, J.P., Virtanen, P., Karhu, H., Salmi, T., Murzin, D.Y., 2006. Supported ionic liquid catalyst (SILCA) in the hydrogenation of citral. Stud. Surf. Sci. Catal. 162, 87–94.

Mehnert, C.P., Mozeleski, J., Cook, R.A., 2002. Supported ionic liquid catalysis investigated for hydrogenation reactions the concept of supported ionic liquid catalysis (silc) has phase and enabled the usage of fixed-bed technology ; the. Chem. Commun. 3010–3011.

Mizuta, R., Murata, A., Ishii, M., Shiogama, H., Hibino, K., Mori, N., Arakawa, O., Imada, Y., Yoshida, K., Aoyagi, T., Kawase, H., Mori, M., Okada, Y., Shimura, T., Nagatomo, T., Ikeda, M., Endo, H., Nosaka, M., Arai, M., Takahashi, C., Tanaka, K., Takemi, T., Tachikawa, Y., Temur, K., Kamae, Y., Watanabe, M., Sasaki, H., Kitoh, A., Takayabu, I., Nakakita, E., Kimoto, M., 2017. Over 5,000 years of ensemble future climate simulations by 60-km global and 20-km regional atmospheric models. Bull. Am. Meteorol. Soc. 98, 1383–1398.

Mohamedali, M., Henni, A., Ibrahim, H., 2019. Investigation of CO2 capture using acetate-based ionic liquids incorporated into exceptionally porous metal–organic frameworks. Adsorption 25, 675–692.

Mohamedali, M., Ibrahim, H., Henni, A., 2018. Incorporation of acetate-based ionic liquids into a zeolitic imidazolate framework (ZIF-8) as efficient sorbents for carbon dioxide capture. Chem. Eng. J. 334, 817–828.

Moya, C., Alonso-Morales, N., Gilarranz, M.A., Rodriguez, J.J., Palomar, J., 2016. Encapsulated ionic liquids for CO2 capture: using 1-Butyl-methylimidazolium acetate for quick and reversible CO2 chemical absorption. ChemPhysChem 17, 3891–3899.

Nanda, S., Reddy, S.N., Mitra, S.K., Kozinski, J.A., 2016. The progressive routes for carbon capture and sequestration. Energy Sci. Eng. 4, 99–122.

Nkinahamira, F., Su, T., Xie, Y., Ma, G., Wang, H., Li, J., 2017. High pressure adsorption of CO2on MCM-41 grafted with quaternary ammonium ionic liquids. Chem. Eng. J. 326, 831–838.

Peng, H.L., Zhong, F.Y., Zhang, J.B., Zhang, J.Y., Wu, P.K., Huang, K., Fan, J.P., Jiang, L.L., 2018. Graphitic carbon nitride functionalized with polyethylenimine for highly effective capture of carbon dioxide. Ind. Eng. Chem. Res. 57, 11031–11038.

Pino, L., Italiano, C., Vita, A., Fabiano, C., Recupero, V., 2016. Sorbents with high efficiency for CO2capture based on amines-supported carbon for biogas upgrading. J. Environ. Sci. (China) 48, 138–150.

Pongstabodee, S., Pornaroontham, P., Pintuyothin, N., Pootrakulchote, N., Thouchprasitchai, N., 2016. CO2capture performance of bi-functional activated bleaching earth modified with basic-alcoholic solution and functionalization with monoethanolamine: isotherms, kinetics and thermodynamics. J. Environ. Sci. (China) 48, 126–137.

Ren, J., Wu, L., Li, B.-G., 2012. Preparation and CO $_2$ sorption/desorption of *N* -(3-Aminopropyl)Aminoethyl tributylphosphonium amino acid salt ionic liquids supported into porous silica particles. Ind. Eng. Chem. Res. 51, 7901–7909.

Rufford, T.E., Smart, S., Watson, G.C.Y., Graham, B.F., Boxall, J., Diniz da Costa, J.C., May, E.F., 2012. The removal of CO2and N2from natural gas: a review of conventional and emerging process technologies. J. Pet. Sci. Eng. 94–95, 123–154.

Safiah, M.N., Azmi, B.M., Normawati, M.Y., 2014. CO2 capture using silica and molecular sieve impregnated with [hmim][Tf2N]. Int. J. Chem. Eng. Appl. 5, 342–346.

Salehi, S., Anbia, M., 2017. High CO $_2$ adsorption capacity and CO $_2$/CH $_4$ selectivity by nanocomposites of MOF-199. Energy Fuels 31, 5376–5384.

Sankar, S., Sharma, S.K., Kaur, N., Lee, B., Kim, D.Y., Lee, S., Jung, H., 2016. Biogenerated silica nanoparticles synthesized from sticky, red, and brown rice husk ashes by a chemical method. Ceram. Int. 42, 4875–4885.

Sawant, D.P., Vinu, A., Jacob, N.E., Lefebvre, F., Halligudi, S.B., 2005. Formation of nanosized zirconia-supported 12-tungstophosphoric acid in mesoporous silica SBA-15: a stable and versatile solid acid catalyst for benzylation of phenol. J. Catal. 235, 341–352.

Sayari, A., Belmabkhout, Y., Serna-Guerrero, R., 2011. Flue gas treatment via CO2adsorption. Chem. Eng. J. 171, 760–774.

Selvakannan, P.R., Mantri, K., Tardio, J., Bhargava, S.K., 2013. High surface area Au-SBA-15 and Au-MCM-41 materials synthesis: tryptophan amino acid mediated confinement of gold nanostructures within the mesoporous silica pore walls. J. Colloid Interface Sci. 394, 475–484.

Song, C., Liu, Q., Ji, N., Deng, S., Zhao, J., Kitamura, Y., 2017. Natural gas purification by heat pump assisted MEA absorption process. Appl. Energy 204, 353–361.

Thouchprasitchai, N., Pintuyothin, N., Pongstabodee, S., 2017. ScienceDirect Optimization of CO 2 adsorption capacity and cyclical adsorption/desorption on tetraethylenepentamine-supported surface-modified hydrotalcite. J. Environ. Sci. 65, 293–305.

Ünveren, E.E., Monkul, B.Ö., Sarıoğlan, Ş., Karademir, N., Alper, E., 2017. Solid amine sorbents for CO2capture by chemical adsorption. Review 3, 37–50.

Vilarrasa-Garcia, E., Moya, E.M.O., Cecilia, J.A., Cavalcante, C.L., Jiménez-Jiménez, J., Azevedo, D.C.S., Rodríguez-Castellón, E., 2015. CO2adsorption on amine modified mesoporous silicas: effect of the progressive disorder of the honeycomb arrangement. Microporous Mesoporous Mater. 209, 172–183.

Welton, T., 1999. Room-temperature ionic liquids. Solvents for synthesis and catalysis. Chem. Rev. 99, 2071–2084.

Xie, W., Hu, L., Yang, X., 2015. Basic ionic liquid supported on mesoporous SBA-15 silica as an efficient heterogeneous catalyst for biodiesel production. Ind. Eng. Chem. Res. 54, 1505–1512.

Yang, N., Wang, R., 2015. Molecular sieve supported ionic liquids as efficient adsorbent for CO2 capture. J. Serb. Chem. Soc. 80, 265–275.

Yang, Q., Zhong, C., 2006. Molecular simulation of carbon dioxide/methane/hydrogen mixture adsorption in metal-organic frameworks. J. Phys. Chem. B 110, 17776–17783.

Ye, Q., Jiang, J., Wang, C., Liu, Y., Pan, H., Shi, Y., 2012. Adsorption of low-concentration carbon dioxide on amine-modified carbon nanotubes at ambient temperature. Energy Fuels 26, 2497–2504.

Yim, J.H., Ha, S.J., Lim, J.S., 2018. Measurement and correlation of CO2solubility in 1-butyl-3-methylimidazolium ([BMIM]) cation-based ionic liquids: [BMIM][Ac], [BMIM][Cl], [BMIM][MeSO4]. J. Supercrit. Fluids 138, 73–81.

Zareiekordshouli, F., Lashanizadehgan, A., Darvishi, P., 2018. Study on the use of an imidazolium-based acetate ionic liquid for CO2capture from flue gas in absorber/stripper packed columns: experimental and modeling. Int. J. Greenhouse Gas Control 70, 178–192.

Zhu, J., He, B., Huang, J., Li, C., Ren, T., 2018. Effect of immobilization methods and the pore structure on CO2separation performance in silica-supported ionic liquids. Microporous Mesoporous Mater. 260, 190–200.

Zhu, J., Xin, F., Huang, J., Dong, X., Liu, H., 2014. Adsorption and diffusivity of CO2 in phosphonium ionic liquid modified silica. Chem. Eng. J. 246, 79–87.

Ziobrowski, Z., Krupiczka, R., Rotkegel, A., 2016. Carbon dioxide absorption in a packed column using imidazolium based ionic liquids and MEA solution. Int. J. Greenhouse Gas Control 47, 8–16.

Zou, B., Hu, Y., Yu, D., Xia, J., Tang, S., Liu, W., Huang, H., 2010. Immobilization of porcine pancreatic lipase onto ionic liquid modified mesoporous silica SBA-15. Biochem. Eng. J. 53, 150–153.